

# Supplemental material for ‘Eliminating object prior-bias from sparse-projection tomographic reconstructions’

September 5, 2021

## Contents

<b>1</b>	<b>An alternate method to compute weights-map</b>	<b>2</b>
<b>2</b>	<b>Links to view our 3D reconstructions</b>	<b>4</b>
<b>3</b>	<b>Detecting new changes directly in the measurements</b>	<b>5</b>
<b>4</b>	<b>Motivation for using multiple eigenspaces</b>	<b>7</b>

# 1 An alternate method to compute weights-map

The value of  $k$  (discussed in Sec.7 of the main paper) is typically dependent on the number of false positives the system can allow in exchange for the detection of more true positives (regions of new changes). It is this choice and not the particular type of dataset that affects the selection of  $k$ . In our work, the chosen  $k$  corresponds to the one that gives minimal tolerance to false positives.

However, in case one wishes to completely avoid the use of this hyper-parameter, one can construct a binary weights-map using an alternate method described below.

1. For the purposes of training, treat one of the previously scanned images as test.
2. Annotate the region of differences between the test and all of the previously scanned images based on domain knowledge.
3. Compute the difference between the pilot reconstruction of the test and its projection onto the eigenspace. Let this spatial map be called ‘error map’.
4. Train a Support Vector Machine (SVM) model to classify patches of this error-map image into one of the two categories: new changes present, new changes absent.
5. Once the trained SVM model is obtained, it can be applied to generate binary weights-map for new test images in the same longitudinal study.
6. Once the binary weights-map  $\mathbf{W}_b$  is obtained, the prior and the pilot can be stitched by  $\mathbf{R} = \mathbf{W}_b(\text{Pilot}) + (1 - \mathbf{W}_b)(\text{Prior})$ . Fig. 1 shows results of this method on 2D okra dataset.

Alternatively, these binary weights can also be used in the below optimization, although this approach has not been pursued here.

$$J_3(\boldsymbol{\theta}, \boldsymbol{\alpha}) = \|\mathcal{R}\mathbf{x} - \mathbf{y}\|_2^2 + \lambda_1 \|\boldsymbol{\theta}\|_1 + \lambda_2 \|\mathbf{W}_b(\mathbf{x} - (\boldsymbol{\mu} + \sum_k \mathbf{V}_k \alpha_k))\|_2^2. \quad (1)$$

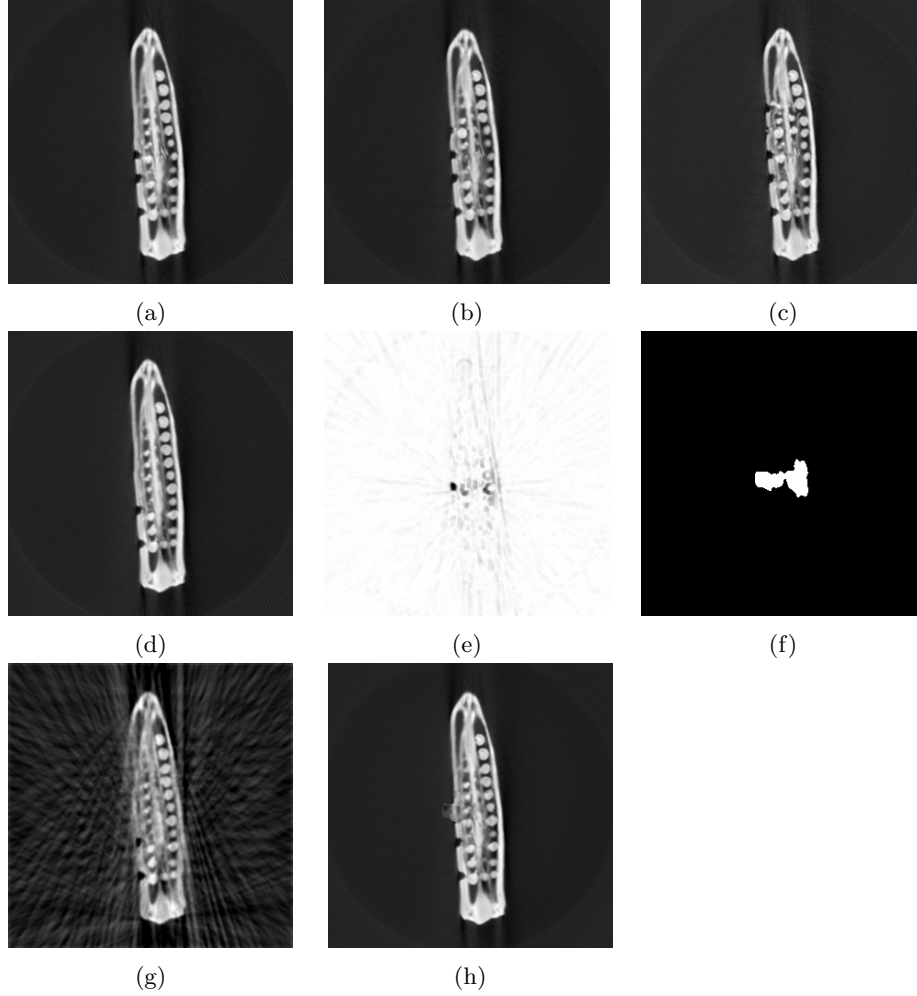


Figure 1: Using an alternate approach to generate (binary) weights map. (a)-(c) the images used as object-prior, (d) the test ( $310 \times 310$ ). Measurements along 60 views were taken. (e) error-map showing new regions, (f) detected binary weights map showing regions of new changes, (g) pilot, (h) final reconstruction with pilot in the new regions, and prior in the other regions.

## 2 Links to view our 3D reconstructions

Reconstructions for the 3D datasets shown in Figs. 3, 4 and 6 in the main paper can be better visualized in the form of a video. Please refer to the following links to view the reconstruction results:

- **Okra:**

<https://www.dropbox.com/sh/vkol8aluzsnusfo/AABtu6-M1LKOsQjKIjxlSxUfa?dl=0>

- **Potato:**

<https://www.dropbox.com/sh/w16j7pvud2lbrpx/AACCJLxgoAurT2vVKIdu-MwFa?dl=0>

- **Sprouts:**

<https://www.dropbox.com/sh/y6s4h2p04tp1lgq/AADn2q43o7SYj10rmheMCDzZa?dl=0>

### 3 Detecting new changes directly in the measurements

Sec.2 of the main paper (‘Related work’) contrasts the spatially-varying technique with other prior based techniques in literature. Here we present a 2D reconstruction result (of the test shown in Figure. 2) to compare our method with [1], in which the new changes are directly detected in the measurement space by computing the difference between the measurements of the test and the corresponding simulated measurements of the template. This difference-volume is then reconstructed and then fused (added to) with the original high quality template. However, in the above method, the sub-sampling artefacts present in the difference-volume gets carried over to the final reconstructed image. This is shown in Figure 3. A quantitative comparison over the region of interest is shown in Table 1.

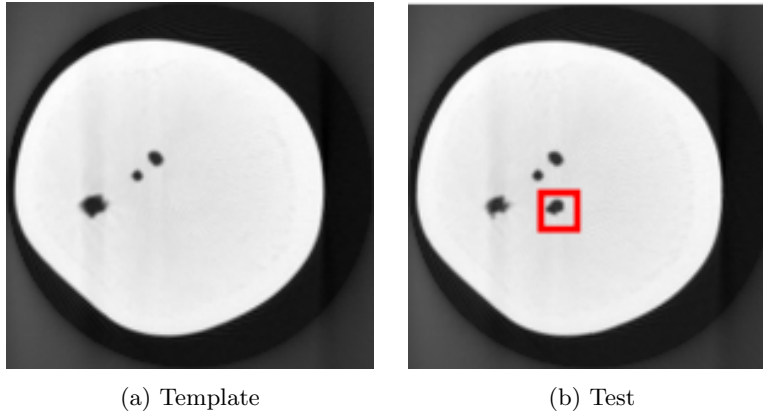


Figure 2: Template and test from the Potato dataset for the reconstructions shown in Figure. 3

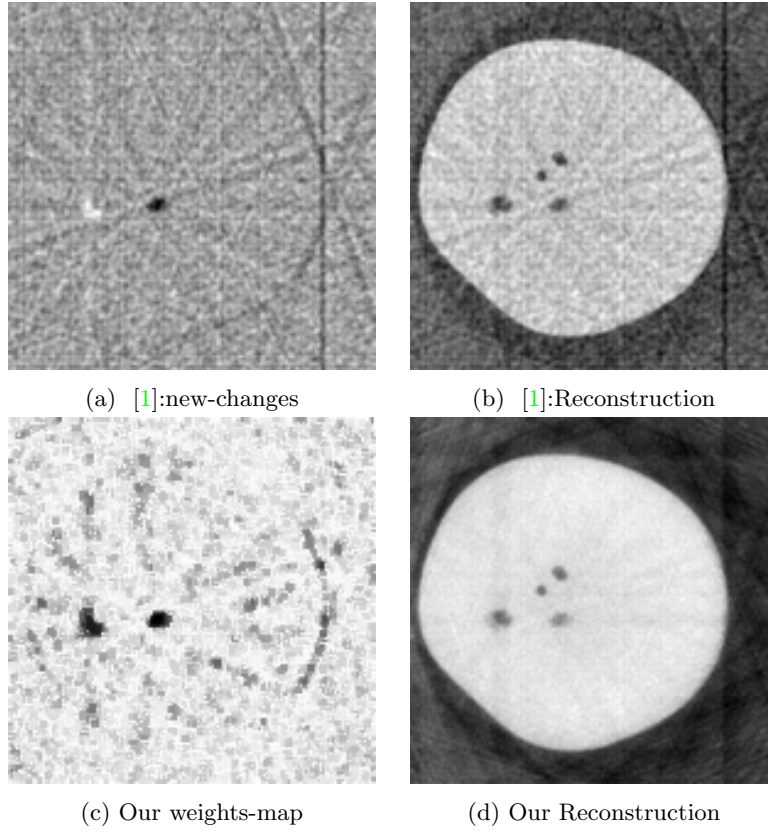


Figure 3: Reconstruction of the test in Figure 2. Reconstructions were performed from 12 views. Gaussian noise of 0 mean and  $SD = 1\%$  of mean of measurements, was added to the measurements.

Table 1: SSIM values (within RoI) of reconstructions shown in Figure 3

	SSIM (whole image)	SSIM (RoI)
Method in [1]	0.65	0.60
Spatially-varying prior	0.89	0.92

## 4 Motivation for using multiple eigenspaces

Here we present a schematic explaining the advantage of using multiple eigenspaces within the proposed spatially-varying reconstruction technique.

**Schematic 1:** Motivation behind our algorithm. (The plus  $\oplus$  and the minus  $\ominus$  operators are placeholders; precise details available in Section 5 of the main paper).

Let  $\text{prior } Q := \text{old regions } (O)$

Let  $\text{test volume } \mathbf{x} := \text{old regions } (O) \oplus \text{new regions } (N)$

1. Compute pilot reconstruction of  $\mathbf{x}$ . Let this be called  $X$ .  
 $X = O \oplus N \oplus Ar(O) \oplus Ar(N)$ , where  
 $Ar(O)$  denote the reconstruction artefacts that depend on the old regions, the imaging geometry and the reconstruction method, and  
 $Ar(N)$  denote the reconstruction artefacts that depend on the new regions, imaging geometry and the reconstruction method.
2. Note that  $Q \ominus X = N \oplus Ar(O) \oplus Ar(N)$  gives the new regions, but along with lots of artefacts due to the imaging geometry (sparse views). To eliminate these unwanted artefacts, compute  $Y = Q \oplus Ar(O)$  by simulating projections from  $Q$  using the same imaging geometry used to scan  $\mathbf{x}$ , and then reconstructing a lower quality prior volume  $Y$ .
3. Note that  $Y \ominus X = N \oplus Ar(N)$  contains the artefacts due to the new regions only. These are different for different reconstruction methods. To eliminate these method dependent artefacts, compute  $Y$  and  $X$  using different reconstruction methods. Let these be denoted by  $Y^j$  and  $X^j$  respectively.
4. Compute
$$\begin{aligned} Y^1 \ominus X^1 &= N \oplus Ar^1(N) \\ Y^2 \ominus X^2 &= N \oplus Ar^2(N) \end{aligned}$$
5. New regions are obtained by computing
$$(Y^1 \ominus X^1) \cap (Y^2 \ominus X^2) = N$$
6. Finally, assign space-varying weights  $\mathbf{W}$  based on step 5.

## References

- [1] J. Lee, J. W. Stayman, Y. Otake, S. Schafer, W. Zbijewski, A. J. Khanna, J. L. Prince, and J. H. Siewerdsen, “Volume-of-change cone-beam CT for image-guided surgery,” pp. 4969–89, Aug 2012.